Increased Sensitivity of Multiwalled Carbon Nanotube Network by PMMA Functionalization to Vapors with Affine Polarity

R. Olejnik,[1,2] P. Slobodian,[1,2] P. Riha,[3] M. Machovsky[1]

[1]*Polymer Centre, Faculty of Technology, T. Bata University in Zlin, 760 01 Zlin, Czech Republic*
[2]*Centre of Polymer Systems, University Institute, T. Bata University, Nad Ovcirnou 3685, 760 01 Zlin, Czech Republic*
[3]*Institute of Hydrodynamics, Academy of Sciences, 166 12 Prague, Czech Republic*

Received 15 March 2011; accepted 10 October 2011
DOI 10.1002/app.36366
Published online in Wiley Online Library (wileyonlinelibrary.com).

ABSTRACT: Multiwalled carbon nanotube network (MWCNT-N)/poly(methyl methacrylate) (PMMA) composite is prepared by solution radical polymerization. The entangled multiwall carbon nanotube network (MWCNT-N) is obtained by vacuum filtration and functionalized by allyl isocyanate to form polymerizable vinyl groups on a nanotube surface. The solution polymerization binds PMMA covalently to these groups and yields MWCNT-N/PMMA composite manifesting electrical conduction and selective chemical vapor sensing. The latter property is evaluated in terms of affinity of organic solvent vapor and PMMA polarities. It is found that the affinity of acetone polarity with polarity of PMMA improves significantly the sensitivity of the composite to this solvent while the sensitivity to methanol is the same and to *iso*-pentane even decreased in comparison with the corresponding property of MWCNT-N. The composite selective response is favorable for a possible composite use as a sensing element and/or vapor switch. © 2012 Wiley Periodicals, Inc. J Appl Polym Sci 000: 000–000, 2012

Key words: poly(methyl methacrylate) nanocomposites; carbon nanotube networks; electrical resistance; vapor sensing; VOC

INTRODUCTION

Carbon nanotube (CNT)/polymer composites are a type of highly promising materials, where specific properties of CNT can be effectively availed serving for a new multifunctional material with enhanced mechanical, thermal, or electrical properties. Recently, there are efforts to apply CNT in polymer composites not as particular filler but as an entangled network. The novel composites may be used not only as a conductive material[1,2] but also as flame retardant,[3,4] electrode,[5] actuator,[6] strain[7] or pressure sensor,[8,9] organic vapor sensor,[9] etc.

Both principal types of CNT—the multiwalled and single-walled nanotubes—show remarkable sensitivity to the change of chemical composition of the surrounding environment. Gas and vapor adsorption as well as desorption usually proceeds at high rates and amounts.[10] This property is favorable for their use in the form of membranes,[11] adsorbents,[12] or gas sensors.[13,14]

The molecules are adsorbed on CNT surface by van der Waals attracting forces. CNT macroscopic forms like aggregates contain four different adsorption sites: internal, interstitial channels, external grooves, and surfaces.[12] The adsorbed molecules influence the electrical properties of isolated CNT and also the resistance of inter-tube contacts.[15,16] The electrical resistance of CNT aggregates or network structures is predominantly determined by contact resistance of crossing tubes rather than by resistance of CNT segments. The tubes are usually much shorter than sensor dimension and inter-tube contacts act as parallel resistors between highly conductive CNT segments. The significant effect which has influence on the macroscopic CNT electrical resistance is a vapor adsorption at the contacts between nanotubes forming non-conductive layers between them.[13] Thus the resistance measurement is a simple and convenient method to register CNT response to vapor action.

Carbon nanotube/PMMA composites can be used as resistive gas sensors for detection of volatile organics compounds. Several principles of sensing mechanisms can be employed as the change of intrinsic resistance of individual tubes fixed in PMMA matrixes by exposure to reducing methanol vapors[17] or in the form of thin polymeric film with percolating CNT network.[18,19] Also a pure network of CNT can be used. In this case, the conductive

Correspondence to: P. Slobodian (slobodian@ft.utb.cz).

PMMA/CNT composite is prepared by dispersion of spray layer by layer of PMMA microbeads decorated by CNT.[20] Here analyzed molecules lead to easy disconnection of conducting path created by CNT network bridging PMMA microbeads.

The aim of this paper is to prepare a pure MWCNT network and MWCNT-N/PMMA composite and test their vapor sensing ability when exposed to solvents of different polarities and vapor pressure. A selection of solvents covering a broad range of polarities thus enables to reveal MWCNT-N and the composite properties which are suitable for its possible application as a sensing element and/or vapor switch.

EXPERIMENTAL

Materials and procedures

The purified MWCNT of acetylene type were supplied by Sun Nanotech Co., China (diameter 10–30 nm, length 1–10 μm, purity >90% and volume resistance 0.12 Ω cm according to supplier). The complete information about the used pristine MWCNT can be found in our paper,[21] where the results of TEM analysis are presented, so that the diameter of individual nanotubes was determined within the range of 10–60 nm (100 measurements), the average diameter and standard deviation 15 ± 6 nm, and the length from tenths of micron up to 3 μm. The tube wall consists of about 15–35 rolled layers of graphene, with the interlayer distance of ca. 0.35 nm.

MWCNT aqueous paste was prepared using a mortar and pestle (1.6 g of MWCNT and ~ 50 ml of deionized water), then diluted by deionized water and SDS (sodium dodecyl sulfate) and 1-pentanol were added, pH was adjusted to the value of 10 using aqueous solution of NaOH.[22] The final nanotubes concentration in the suspension was 0.3 wt %, concentrations of SDS and 1-pentanol were 0.1 *M* and 0.14 *M*, respectively.[23] The dispersion was homogenized using Dr. Hielscher GmbH apparatus (ultrasonic horn S7, amplitude 88 μm, power density 300 W/cm^2, frequency 24 kHz) for 2 h at the temperature of ca. 50°C. MWCNT networks were prepared by dispersion vacuum filtration through nonwoven polyurethane porous membrane (SPUR a.s, Czech Republic). The membrane was made by electrospinning from PU dimethyl formamide (DMF) solution. For more details of PU chemical composition and particular process characteristics see Refs. 8 and 24. The formed disk-shaped MWCNT network was washed several times by deionized water and methanol in situ, then removed and dried between filter papers at room temperature.

MWCNT-N/PMMA composite was prepared by solution radical polymerization. MWCNT-N was initially functionalized by allyl isocyanate (3 wt % of DMF anhydrous allyl isocyanate solution) at 70°C for 18 h to synthesize free polymerizable vinyl groups on CNT surface. The functionalized network was then put to polymerization glass reactor containing solution of methyl methacrylate (MMA) in methylethyl ketone (MEK) (40 wt %) with a solved azobisisobutyronitrile (AIBN) as radical initiator (1 wt % calculated on total monomer content). The networks made from functionalized and pristine nanotubes were polymerized at 70°C for 20 h. The networks were repeatedly immersed into MEK after polymerization for 30 min to dissolve un-grafted molecules (concentration of MWCNT-N in MEK was around 0.1 wt %) and dried at 40°C for 2 days. Pure PMMA was prepared under the same condition of polymerization as composites, that is, MMA in MEK (40 wt %) polymerized at 70°C for 20 h.

Measurement and characterization

The structure of networks was investigated by a scanning electron microscope (SEM) made by Vega LMU (Tescan s.r.o., Czech Republic). The network was deposited on the carbon targets and covered with a thin Au/Pd layer. For the observations, the regime of secondary electrons was chosen.

Pure MWCNT were also analyzed via transmission electron microscopy (TEM) using microscope JEOL JEM 2010 at the accelerating voltage of 160 kV. The sample for TEM was prepared on 300 mesh copper grid with a carbon film (SPI) from MWCNT dispersion in acetone which was prepared by ultrasonication, deposited on the grid and dried.

Thermogravimetric analysis (TGA) of the samples was carried out using thermogravimeter Setaram Setsyt Evolution 1200. The samples were examined under inert atmosphere of helium (5.5 purity, SIAD TP); the gas flow was 30 cm^3/min at the pressure of 101.325 kPa (i.e., 30 sccm) for all experiments. A platinum crucible was used for the sample, the weight of which was about 4 mg. The temperature was continually increased from the ambient temperature up to 1200°C at the rate of 20°C/min. The calorimetric analysis of MWCNT-N/PMMA composite was performed using differential scanning calorimeter (Perkin-Elmer). The reason was to check thermal properties of synthesized PMMA on CNT surface. To maximize the response from the polymer, the composite was annealed at temperature below PMMA glass transition temperature T_g and again gradually heated.[25] The exact procedure was following. The composite was annealed at 220°C for 5 min, cooled to 100°C at the cooling rate of 10°C/min, isothermal relaxation at 100°C for 1000 min was performed, cooled to 50°C at the cooling rate of 10°C/min and for 1 min annealed at 50°C. The proper

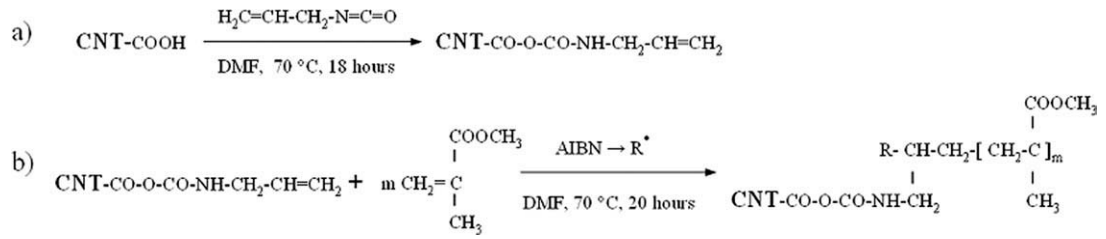

Figure 1 Synthetic route used to prepare MWCNT-N/PMMA composite. a) Reaction of carboxylic group of CNT with binder (allyl isocyanate); b) radical polymerization-incorporation of free vinyl group bonded to the surface of CNT into PMMA growing chain. R denotes radical created from initiator of polymerization AIBN—azobisisobutyronitrile (isobutyronitrile-free radical).

measurement was done in the course of increasing temperature up to 220°C at the heating rate 10°C/min. The similar measurement to illustrate the physical aging phenomenon in pure PMMA was performed when PMMA specimen was annealed at 90°C for 60 and 600 h before DSC up scan.

The electrical resistance of network stripes cut out from the manufactured MWCNT-N and MWCNT-N/PMMA disks (length 15 mm, width 5 mm, thickness ca. 0.3 mm) was measured along the specimen length by the two-point technique using multimeter Sefram 7338. The stripe was placed on a planar holder with Cu electrodes fixed on both sides of the specimen. Time-dependent electrical resistance measurements were performed during adsorption and desorption cycles. In the former case, the holder with the specimen was quickly transferred into an airtight conical flask full of vapors of the respective solvent (*iso*-pentane, acetone, and methanol), a layer of which was at the bottom. The measurements were conducted in saturated vapors at atmospheric pressure, temperature 25°C and relative humidity 60%.[26,27] After 6 min of measurement, the holder was promptly removed from the flask and for the next 6 min the sample was measured in the mode of desorption. This was repeated five times in consecutive cycles.

RESULTS

Structure and properties

A principle of synthetic route used to prepare MWCNT/PMMA nanocomposite is presented in Figure 1. There are two steps of MWCNT functionalization when natural groups presented on surface of CNT (created by CNT postproduction air oxidation) like carboxylic groups (presented in the scheme) but also hydroxyls react with a binder (allyl isocyanate) and create a covalent bond with CNT. Thereafter, a free vinyl group of functionalized CNT is incorporated into growing PMMA chain in the course of radical polymerization of MMA monomer in solution. R in Figure 1 represents the isobutyronitrile-free radical created by thermal decomposition of used radical initiator (AIBN—azobisisobutyronitrile).

The prepared free-standing MWCNT-N of disk shape is shown in Figure 2a. The disk was uniform, smooth, and crack-free, with significant structural integrity allowing easy manipulation. The typical thickness was in the range of 0.15–0.65 mm according to the volume of aqueous MWCNT dispersion used in filtration. The second part of Figure 2 shows SEM micrograph of MWCNT-N surface (Buckypaper) made of entangled tubes. The network porosity $\phi = 0.67$ was calculated through the relation $\phi = 1 - \rho_{net}/\rho_{MWCNT}$, where $\rho_{net} = 0.56 \pm 0.03$ g/cm^3 denotes the measured apparent density of the nanotube network and $\rho_{MWCNT} = 1.7$ g/cm^3 denotes density of nanotubes. The density of nanotube network, ρ_{net}, was calculated from the data obtained by weighting and measuring the network strips. The density of nanotubes was determined by means of the rule of mixing from the measured densities of PMMA/CNT composites (0, 0.5, 1.0 wt % of CNT) prepared by precipitation of their methyl-ethyl ketone solutions pouring into water.[28] Both principal materials are electrical conductive with measured electrical resistivity of MWCNT-N 0.078 ± 0.003 Ω cm and 0.094 ± 0.008 Ω cm for MWCNT-N/PMMA composite.

MWCNT-N was functionalized by allyl isocyanate to synthesize free polymerizable vinyl groups on CNT surface and bind PMMA to these groups. The

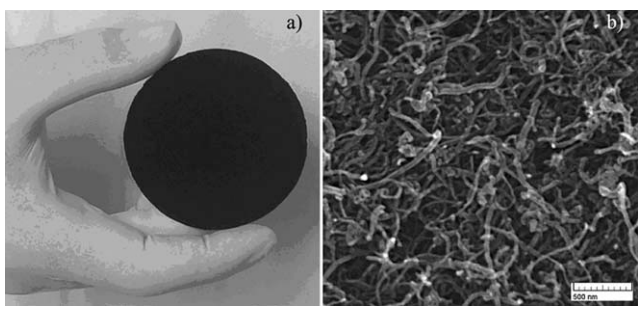

Figure 2 Free-standing randomly entangled MWCNT network (disk diameter 75 mm, thickness 0.15 mm) (a), and SEM image of the surface of entangled MWCNT-N network made of pure MWCNT (b).

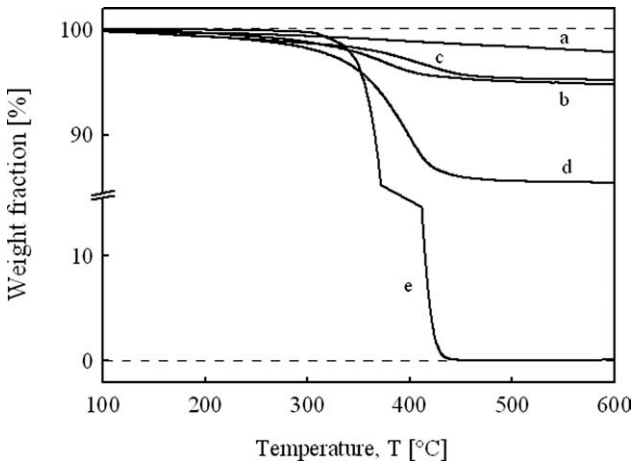

Figure 3 Thermogravimetric analysis of pristine MWCNT (a), allyl isocyanate functionalized MWCNT-N (b), MWCNT-N/PMMA network nanocomposite prepared by only solution polymerization (c), MWCNT-N/PMMA network prepared by solution radical polymerization of allyl isocyanate functionalized MWCNT-N (d), and PMMA (e).

reason was to change MWCNT-N affinity to molecules of organic solvent vapors. The quantity of organic molecules bound to the network was determined by means of thermogravimetric (TG) analysis. The results are presented in Figure 3 where MWCNT-N made of pristine nanotubes shows hardly any degradation in the range of temperatures used (up to 700°C); only very small mass loss of ca. 3 wt % was observed at the highest temperature. This is probably caused by decomposition of amorphous carbon contained in the original material together with functional groups like O—C=O or C—O, also included in crude material. On the other hand, the main chain of PMMA starts to decay at the temperature of about 300°C and is totally decomposed at some 450°C (curve e). The decomposition for PMMA-grafted composite is between 260 and 530°C with maximum at 400°C (curve c) and for allyl functionalized MWCNT-N between 320 and 550°C (curve b). The amount of bonded organic molecules to MWCNT-N was determined as the difference in residual weights of MWCNT-N and composite. The calculated value was about 3 wt % for both allyl isocyanate functionalized MWCNT-N and MWCNT-N/PMMA composite prepared by solution polymerization and 13 wt % for MWCNT-N/PMMA network nanocomposite prepared by solution polymerization of allyl isocyanate functionalized MWCNT-N.

The organic molecules in case of the allyl functionalized composite originate from covalently bonded allyl isocyanate molecules by reaction of isocyanate group with functional groups presented on the surface of CNT. In the case of grafted composite, the CNT surface is functionalized by the radicals originated during polymerization process. The free radicals created either from the initiator or as a growing polymer macro-radicals are able to react with CNT structure by opening the π-bonds in carbon nanotubes and creating a covalent bond between CNT and the radicals (radical addition).[29,30] In the case of MWCNT-N/PMMA network composite prepared by solution polymerization of allyl isocyanate functionalized MWCNT-N, the loss value represents the molecules covalently bonded to CNT surface by radical addition and/or incorporation of free allyl groups attached to CNT surface. Also some portion of isobutyronitrile groups originated from radical initiator AIBN should be expected to be covalently bonded to CNT surface again by process of radical addition.[29] The detected value around 13 wt % is lower in comparison with 45 wt % of PS,[31] or 47 wt % of PMMA[32] for the same technique using isocyanate-based binding elements followed by radical polymerization. The cause is probably less functional groups on CNT surface like acid groups (—COOH) and hydroxyl groups (—OH) capable of reaction with isocyanate groups. Even though the pristine CNT have some functional groups appearing immediately after the CNT production, another groups originate at the proper CNT oxidation when they are exposed to air environment.[33] In this work, pure and non-treated tubes were used contrary to oxidized CNT (by mixture of sulfuric and nitric acids) in[31,32] what means a limited number of sites for potential isocyanate-based linking.

The TEM images of MWCNT structure from MWCNT-N/PMMA composite are presented in Figure 4. The TEM micrographs clearly confirm the presence of PMMA adhering to the MWCNT surface in the form of so-called polymeric "brushes."[31] The polymeric material is found to create discontinuous coverage, part a, or a continuous layer, part b. The approximate thickness is around 1.6 nm in part a and 3–4 nm in part b, which is similar to published values of 4–5 nm.[31,34]

Differential scanning calorimetry analysis of MWCNT-N/PMMA indicates the presence of PMMA bonded to CNT when glass transition region of PMMA defined by a glass transition temperature is reached (Fig. 5). There was measured a broad transition peak during composite heating which overlaps the instrument baseline between ~110 and 155°C (T_g, onset ~ 120°C) after 1000 h of relaxation at 100°C. The measured enthalpy of transition from glass to melt was ~ 0.3 J/g. The annealing was chosen to increase the amount of thermal response during composite heating by the effect of "physical aging phenomenon"[25] occurring in non-crystalline solids like amorphous PMMA. Also it was found that the transition enthalpy increases with time of annealing which suggests again that organic material determined by TG analyses is mostly PMMA. The glass transition temperature of PMMA is usually reported to be

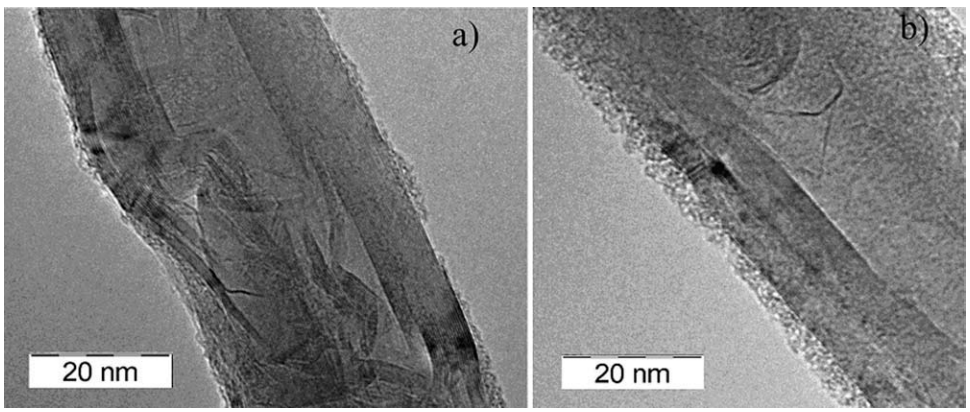

Figure 4 TEM analyses of individual MWCNT tube from MWCNT-N/PMMA network prepared by solution radical polymerization of allyl isocyanate functionalized MWCNT-N, PMMA "brushes" on MWCNT surface.

around 105°C (determined as the transition peak maximum) and transition extension reaches some 16°C. The difference in thermal properties of bulk PMMA compared to PMMA in the composite can be explained by the polymer segment immobilization on the surface of CNT. This phenomenon is usually reported to change thermal properties of polymeric materials such as an increase in T_g and broadening of T_g region.[35] The same phenomenon of physical aging occurs in pure PMMA presented in figure by full symbols (T_g, onset ~96°C, enthalpy of transition 2.1 J/g after 600 h of annealing at 90°C).

The chemical treatment of MWCNT network by allyl isocyanate and subsequent polymerization significantly changes network structure. It is shown in the micrographs of treated MWCNT-N and MWCNT-N/PMMA composite in Figure 6. The surface of the functionalized network seems smooth with grains which indicates that some nanotubes were deposited in agglomerates rather than individually during the network formation. On other hand, the surface of MWCNT-N/PMMA composite is wrinkled and large aggregates can be seen. The reason is probably local network shrinkage in the course of polymerization process when the contraction of PMMA during polymerization of MMA affects also network structure. The effect of polymerization on the composite structure is obvious from the micrographs of the network cross-section in Figure 7. The functionalized MWCNT-N consists of entangled tubes whereas the structure of MWCNT-N/PMMA is distorted by a local shrinkage. Moreover, PMMA seems to form porous texture rather than a continuous polymeric matrix.

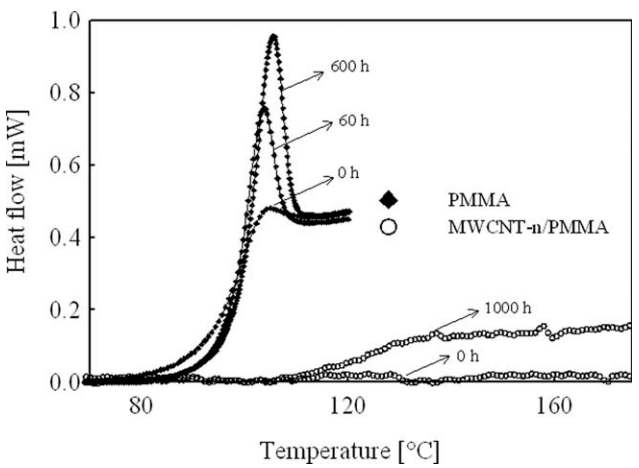

Figure 5 Differential scanning calorimetry analysis of PMMA and MWCNT-N/PMMA composite prepared by solution radical polymerization of allyl isocyanate functionalized MWCNT-N. The enhancement of glass transition response measured at DCS up-scan by process of physical aging of specimens at annealing temperatures below T_g. PMMA annealed at 90°C for 60 and 600 h and the composite at 100°C for 1000 h.

The SEM pictures of upper surface of pure MWCNT-N and MWCNT-N/PMMA composite were used for determination of the pore size distribution by means of the recently proposed digital image analysis technique.[36] The distributions are plotted in Figure 8 and show that the pure MWCNT-N has pores between 9.4 and 611 nm while

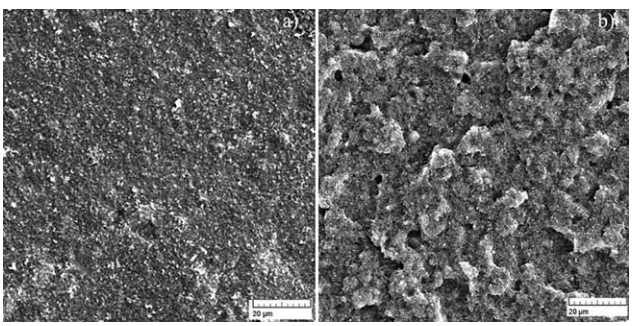

Figure 6 SEM analyses of the upper surfaces of MWCNT-N (a) and MWCNT-N/PMMA nanocomposite (b) prepared by solution radical polymerization of allyl isocyanate functionalized MWCNT-N.

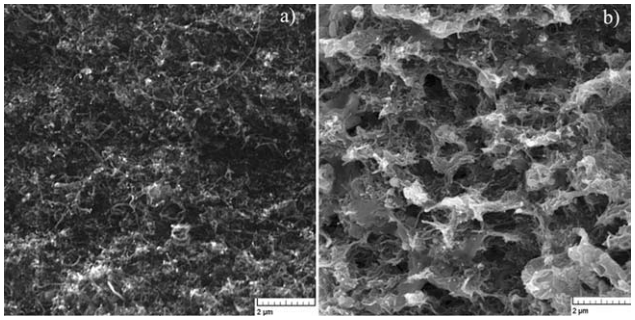

Figure 7 SEM analyses of the fracture surface of MWCNT-N (a) and MWCNT-N/PMMA nanocomposite (b) prepared by solution radical polymerization of allyl isocyanate functionalized MWCNT-N.

MWCNT-N/PMMA composite has larger pores in the range between 28 and 1840 nm.

Vapor sensing properties

Iso-pentane (*i*-PE), acetone, and methanol were used for the investigation of vapor sensing properties of nanotube networks. The chosen solvents cover a broad range of Hansen solubility parameters. The values for acetone are very close to PMMA values while *i*-PE is non-polar and methanol is on the other hand polar solvent but both do not solve PMMA. The data are presented in Table I and Figure 9. The parameters are defined by

$$\delta_t{}^2 = \delta_d{}^2 + \delta_p{}^2 + \delta_h{}^2 \tag{1}$$

where δ_t is the total Hildebrand solubility parameter, and δ_d, δ_p, and δ_h denotes the dispersion, the polar, and the hydrogen bonding component, respectively. The fractional parameters for the Teas triangular graph are defined as

$$\begin{array}{ll} f_d = \delta_d/\left(\delta_d + \delta_p + \delta_h\right), & f_p = \delta_p/\left(\delta_d + \delta_p + \delta_h\right), \\ f_h = \delta_h/\left(\delta_d + \delta_p + \delta_h\right), & f_d + f_d + f_h = 100. \end{array} \tag{2}$$

The values of fractional parameters for acetone are very similar to the value for PMMA, that is, acetone: $f_d = 47.1\%$, $f_p = 31.6\%$, and $f_h = 21.3\%$) and PMMA: $f_d = 50.8\%$, $f_p = 28.7\%$, and $f_h = 20.5\%$. The parameters for *i*-PE are $f_d = 100.0\%$, $f_p = 0.0\%$, and $f_h = 0.0\%$ and for methanol $f_d = 30.4\%$, $f_p = 24.8\%$, and $f_h = 44.9\%$. The networks were exposed to vapor of solvent at the saturated vapor pressure p_i and the corresponding volume fraction x_i,

$$x_i = p_i/p_{\mathrm{A}} \tag{3}$$

where p_A denotes the air pressure. The saturated vapor pressure p_i of the used solvents systematically decreases with increasing δ_t (Table I).

The adsorption of solvent molecules by the network increases its electrical resistance and thus the network resistance measurement is a simple and convenient method to register CNT response to vapor action. The vapor network sensitivity may be defined as

$$S = \left(R_g - R_a\right)/R_a = \Delta R/R_a \tag{4}$$

where R_a represents the stripe resistance in the air, and R_g the resistance of network stripe exposed to vapor.

The average sensitivity values for five different MWCNT-N and MWCNT-N/PMMA networks in the course of adsorption/desorption 6-min cycles when exposed to acetone vapors are shown in Figure 10. The mechanism of macroscopic resistance increase can be explained by formation of a non-conducting layer between nanotubes which degrades the quality of inter-tube contact. Desorption cycle starts by a rapid sensitivity decrease followed by a slower decrease to a constant value within the time of cycle. The organic molecules are removed in the course of desorption and the specimen resistance recovers the initial value. The data show higher vapor detection sensitivity of MWCNT-N/PMMA composite (the average sensitivity is 33.3 ± 3.1) than MWCNT network (15.6 ± 0.8). The increased sensitivity of composite is probably due to PMMA which increases the affinity of the composite structure to acetone vapors. The data demonstrates also good reversibility and reproducibility of adsorption/desorption cycles in case of the composite. On the other hand, the residual sensitivity change can be

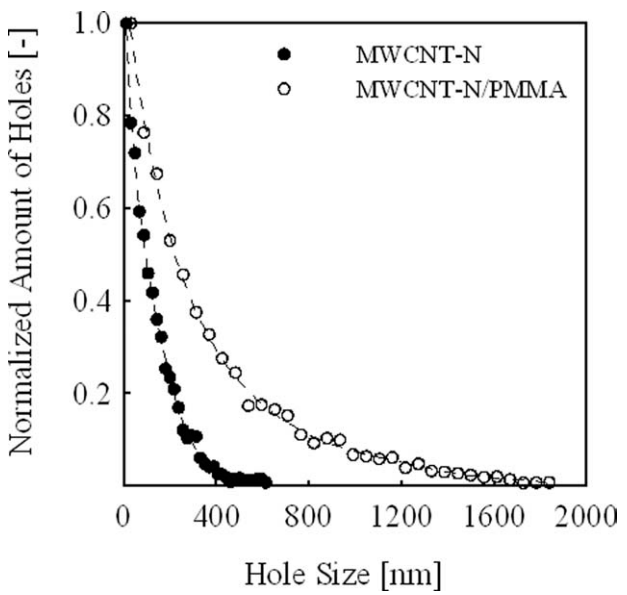

Figure 8 The pore size distribution of pure MWCNT-N and MWCNT-N/PMMA composite prepared by solution radical polymerization of allyl isocyanate functionalized MWCNT-N.

TABLE I
Properties of Tested Organic Solvents and PMMA: Hansen Solubility Parameters δ_d, δ_p, δ_h, Total Hildebrand Solubility Parameter δ_t, Saturated Vapor Pressures p_i, and Corresponding Volume Fractions at 25°C and Atmospheric Pressure x_i

Organic solvent	δ_d (MPa$^{1/2}$)	δ_p (MPa$^{1/2}$)	δ_h (MPa$^{1/2}$)	δ_t (MPa$^{1/2}$)	p_i (kPa)	x_i (vol. %)
PMMA	18.6	10.5	7.5	22.6	–	–
iso-pentane	13.7	0	0	13.7	91.37	90.2
Acetone	15.5	10.4	7.0	20.0	30.46	30.1
Methanol	15.1	12.3	22.3	29.6	16.76	16.5

observed in case of MWCNT-N. The change is probably caused by destruction of some contacts between crossing nanotubes in MWCNT network.[13] The error bars show higher scatter of data for MWCNT-N/PMMA composite than for MWCNT-N. The reason is probably the variability of composite texture compared to pure MWCNT network.

The comparison of network sensitivity for three different solvents (*iso*-pentane, acetone, and methanol) in the typical (third) adsorption/desorption cycle of the cycle sequence is presented in Figure 11. The reached sensitivity values after 6 min of adsorption are listed in Table II together with the ratios of the composite (S_2) to pure MWCNT network sensitivity (S_1). As follows from Figure 11 and Table II, MWCNT-N/PMMA composite is less sensitive when exposed to vapors of *iso*-pentane compared to sensitivity of pure MWCNT-N. The corresponding relation S_2/S_1 is 0.6. Nearly the same response for MWCNT-N and MWCNT-N/PMMA composite is observed for methanol, $S_2/S_1 = 1.1$. However, the significant ratio S_2/S_1 change is found when the composite is exposed to acetone vapor, $S_2/S_1 = 2.1$.

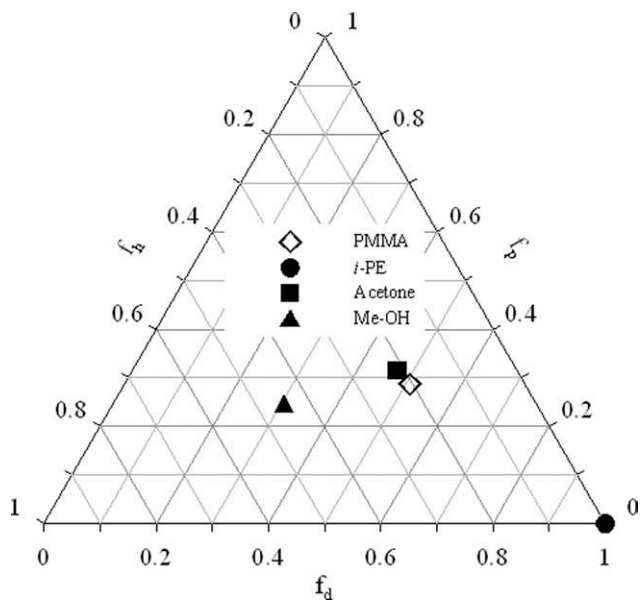

Figure 9 The triangular graph of dispersion, polar, and hydrogen bonding fractional solubility parameters, f_d, f_p, f_h, for used solvents and PMMA.

The main reason is the affinity of PMMA to acetone but the influence of the higher network porosity of composite compared to the one of pure MWCNT-N network cannot be ruled out.

As follows from Figure 11, the network sensitivity depends on the type of network, the vapor pressure and the polarity of the solvent. Figure 12 demonstrates that the maximal sensitivity of pure MWCNT-N increases with volume fraction of vapors x_i despite solvent different polarities. A completely different behavior holds for MWCNT-N/PMMA composite. The composite maximal sensitivities are significantly influenced by the origin of vapors, i.e., their affinity to PMMA. In this respect, the affinity of acetone polarity with polarity

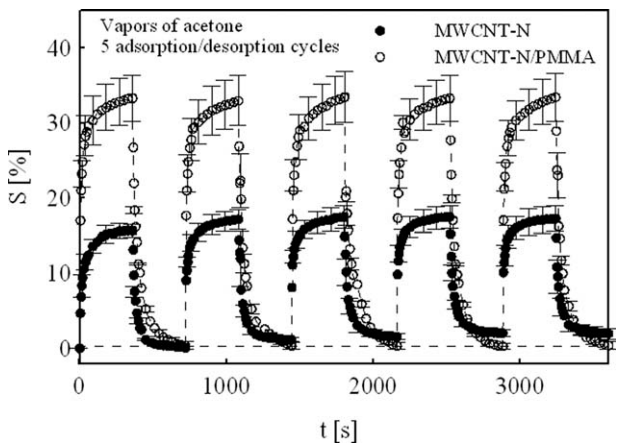

Figure 10 Five adsorption/desorption cycles for MWCNT-N (filled symbols) and MWCNT-N/PMMA nanocomposite (open symbols) prepared by solution radical polymerization of allyl isocyanate functionalized MWCNT-N exposed to vapor of acetone ($n = 5$).

TABLE II
Sensitivities of Both CNT Networks Exposed to Saturated Vapors of Three Different Organic Solvents

Organic solvent	S_1 (%) MWCNT-N	S_2 (%) MWCNT-N/PMMA	S_2/S_1
iso-pentane	20.3 ± 0.6	12.6 ± 1.4	0.6
Acetone	15.6 ± 0.8	33.3 ± 3.1	2.1
Methanol	13.6 ± 0.3	14.7 ± 1.8	1.1

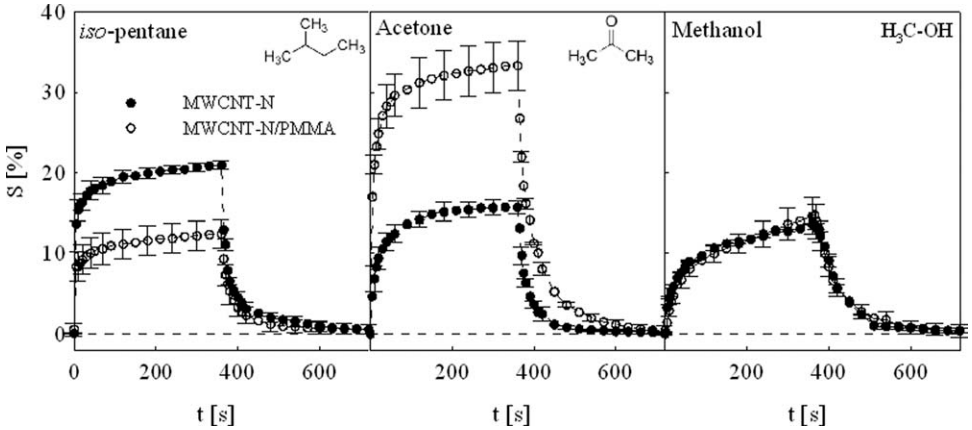

Figure 11 One adsorption/desorption cycle for MWCNT-N (filled symbols) and MWCNT-N/PMMA nanocomposite (open symbols) prepared by solution radical polymerization of allyl isocyanate functionalized MWCNT-N exposed to three different organic solvents: *iso*-pentane (a), acetone (b), and methanol (c).

of PMMA improves significantly the selectivity of the composite network to this solvent while the composite sensitivity to methanol is the same and to *iso*-pentane even lower in comparison with the MWCNT-N sensitivity.

CONCLUSION

Multiwall carbon nanotubes were used to prepare the entangled network and the entangled network/PMMA composite whose response to three organic solvent vapors (*iso*-pentane, acetone, and methanol) was monitored by measuring their electrical resistance change. The resistance response of samples to physisorption and desorption of organic vapors during the test cycles was reversible, reproducible, sensitive, and selective. The possible mechanism of resistance change may involve formation of nonconducting layer between nanotubes in solvent vapors which degrades the quality of inter-tube contact. The nanotube PMMA functionalization improves their sensitivity for acetone vapors. The improvement is caused by affinity of acetone vapors polarity with polarity of PMMA in the composite structure. The potential composite use may be for cheap and easy to prepare micro-sized sensing elements and vapor switches.

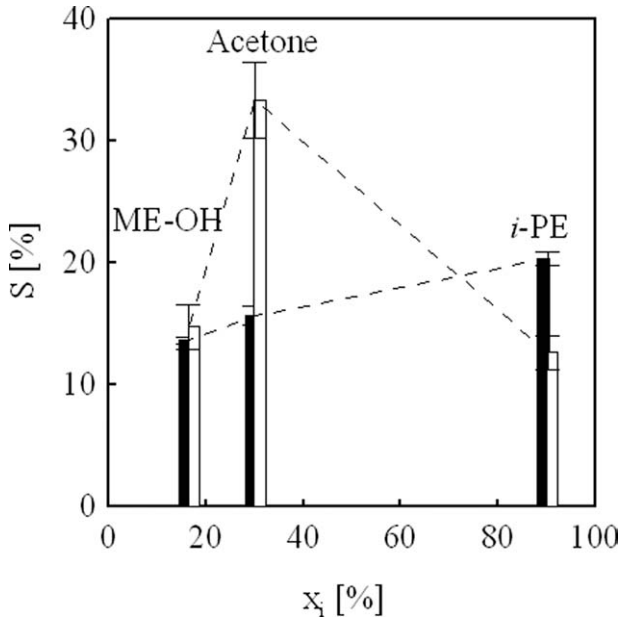

Figure 12 Dependence of sensitivity of MWCNT-N and MWCNT-N/PMMA composite prepared by solution radical polymerization of allyl isocyanate functionalized MWCNT-N on the volume fraction of organic solvent during adsorption/desorption cycle. Black columns are for the pure MWCNT-N sensitivity S_1 and white columns for MWCNT-N/PMMA composite sensitivity S_2.

This project was supported by the internal grant of TBU in Zlín No. IGA/12/FT/11/D funded from the resources of specific university research. This article was also created with the support of Operational Programme Research and Development for Innovations co-funded by the European Regional Development Fund (ERDF) and national budget of the Czech Republic within the framework of the Centre of Polymer Systems project (reg.number: CZ.1.05/2.1.00/03.0111), by the Czech Ministry of Education, Youth and Sports project (MSM 7088352101) and by the Fund of the Institute of Hydrodynamics AV0Z20600510.

The authors would like to thank Dr. Radko Novotny of Palacky University, Olomouc, Czech Republic, for conducting of TEM analyses and Prof. Martin Zatloukal of TBU for performing SEM digital image analysis.

References

1. Cheng, Q. F.; Bao, J. W.; Park, J.; Liang, Z.Y.; Zhang, C.; Wang, B. Adv Funct Mater 2009, 19, 3219.
2. Wang, D.; Song, P. C.; Liu, C. H.; Wu, W.; Fan, S. S. Nanotechnology 2008, 19, 1.
3. Wu, Q.; Zhu, W.; Zhang, C.; Liang, Z.Y.; Wang, B. Carbon 2010, 48, 1799.

4. Fu, X.; Zhang, C.; Liu, T.; Liang, R.; Wang, B. Nanotechnology 2010, 21, 235701.
5. Meng, C. Z.; Liu, C. H.; Fan, S. S. Electrochem Commun 2009, 11, 186.
6. Yun, Z. H.; Shanov, V.; Schulz, M. J.; Narasimhadevara, S.; Subramaniam, S.; Hurd, D.; Boerio, F. J. Smart Mater Struct 2005, 14, 1526.
7. Kang, I. P.; Schulz, M. J.; Kim, J. H.; Shanov, V.; Shi, D. L. Smart Mater Struct 2006, 15, 737.
8. Slobodian, P.; Riha, P.; Lengalova, A.; Olejnik, R.; Saha, P. J Exp Nanosci 2011, 6, 294.
9. Olejnik, R.; Slobodian, P.; Riha, P.; Saha, P. Polym Test (Submitted).
10. Hussain, C. M.; Saridara, C.; Mitra, S. J Chromatogr A 2008, 1185, 161.
11. Smajda, R.; Kukovecz, A.; Konya, Z.; Kiricsi, I. Carbon 2007, 45, 1176.
12. Agnihotri, S.; Mota, J. P. B.; Rostam-Abadi, M.; Rood, M. J. J Phys Chem B 2006, 110, 7640.
13. Romanenko, A. I.; Anikeeva, O. B.; Kuznetsov, V. L.; Buryakov, T. I.; Tkachev, E. N.; Usoltseva, A. N. Sensor Actuat A-Phys 2007, 138, 350.
14. Qureshi, A.; Kang, W. P.; Davidson, J. L.; Gurbuz, Y. Diam Relat Mater 2009, 18, 1401.
15. Tournus, F.; Latil, S.; Heggie, M. I.; Charlier, J. C. Phys Rev B 2005, 72, 075431.
16. Mowbray, D. J.; Morgan, C.; Thygesen, K. S. Phys Rev B 2009, 79, 195431.
17. Li, Y; Wang, H. C.; Yang, M. J. Sensor Actuat B-Chem 2007, 121, 496.
18. Shang, S. M.; Li, L.; Yang, X. M.; Wei, Y. Y. Compos Sci Technol 2009, 69, 1156.
19. Abraham, J. K.; Philip, B.; Witchurch, A.; Varadan, V. K.; Reddy, C. C., Smart Mater Struct 2004, 13, 1045
20. Feller, J. F.; Lu, J.; Zhang, K.; Kumar, B.; Castro, M.; Gatt, N.; Choi, H. J. J Mater Chem 2011, 21, 4142.
21. Slobodian, P.; Riha, P.; Lengalova, A.; Saha, P. J Mater Sci 2011, 46, 3186.
22. Ham, H. T.; Choi, Y. S.; Chung I. J. Colloid Interf Sci 2005, 286, 216.
23. Chern, C. S.; Wu, L. J. J Polym Sci Part A: Polym Chem 2001, 39, 3199.
24. Kimmer, D.; Slobodian, P.; Petras, D.; Zatloukal, M.; Olejnik, R.; Saha P. J Appl Polym Sci 2009, 111, 2711.
25. Slobodian, P.; Riha, P.; Lengalova, A.; Hadac, J.; Saha, P.; Kubat, J. J Non-Cryst Solids 2004, 344, 148.
26. Niu, L.; Luo, Y. L.; Li, Z. Q. Sensor Actuat B-Chem 2007, 126, 361.
27. Slobodian, P.; Riha, P.; Lengalova, A.; Svoboda, P.; Saha, P. Carbon 2011, 49, 2499.
28. Slobodian, P.; Kralova, D.; Lengalova, A.; Novotny, R.; Saha, P. Polym Compos 2010, 31, 452.
29. Wang, X. B.; Li, S. Q.; Xu, Y.; Wan, L.; You, H. J.; Li, Q.; Wang, S. M. Appl Surf Sci 2007, 253, 7435.
30. Kim, S. T.; Choi, H. J.; Hong, S. M. Colloid Polym Sci 2007, 285, 593.
31. Ha, J. U.; Kim, M.; Lee, J.; Choe, S.; Cheong, I. W.; Shim, S. E. J Polym Sci Part A Polym Chem 2006, 44, 6394.
32. Olejnik, R.; Liu, P. B.; Slobodian, P.; Zatloukal, M.; Saha, P. Novel Trends Rheol III 2009, 1152, 204.
33. Rasheed, A.; Howe, J. Y.; Dadmun, M. D.; Britt, P. F. Carbon 2007, 45, 1072.
34. Kim, M. H.; Hong, C. K.; Choe, S.; Shim, S. E. J Polym Sci Part A Polym Chem 2007, 45, 4413.
35. Slobodian, P.; J Therm Anal Calorim 2008, 94, 545.
36. Sambaer, W.; Zatloukal, M.; Kimmer, D. Polym Test 2010, 29, 82.